Experimental realization of crossover in shape and director field of nematic tactoids

Vida Jamali,[1,*] Natnael Behabtu,[1,*] Bohdan Senyuk,[1,2] J. Alex Lee,[1] Ivan I. Smalyukh,[2,3,4]
Paul van der Schoot,[5,6] and Matteo Pasquali[1,7,†]

[1]*Department of Chemical and Biomolecular Engineering, Rice University, Houston, Texas 77005, USA*
[2]*Department of Physics, University of Colorado at Boulder, Boulder, Colorado 80309, USA*
[3]*Department of Electrical, Computer, and Energy Engineering and Materials Science and Engineering Program, and Liquid Crystals Materials Research Center, University of Colorado at Boulder, Colorado 80309, USA*
[4]*Renewable and Sustainable Energy Institute, National Renewable Energy Laboratory and University of Colorado, Boulder, Colorado 80309, USA*
[5]*Polymer Physics Group for Theory of Polymers and Soft Matter Group, Department of Applied Physics, Eindhoven University of Technology, P.O. Box 513, 5600 MB Eindhoven, The Netherlands*
[6]*Institute for Theoretical Physics, Utrecht University, Leuvenlaan 4, 3584 CE Utrecht, The Netherlands*
[7]*Department of Chemistry, Department of Materials Science and NanoEngineering, The Smalley Institute for Nanoscale Science and Technology, Rice University, Houston, Texas 77005, USA*

(Received 28 January 2015; published 27 April 2015)

Spindle-shaped nematic droplets (tactoids) form in solutions of rod-like molecules at the onset of the liquid crystalline phase. Their unique shape and internal structure result from the interplay of the elastic deformation of the nematic and anisotropic surface forces. The balance of these forces dictates that tactoids must display a continuous variation in aspect ratio and director-field configuration. Yet, such continuous transition has eluded observation for decades: tactoids have displayed either a bipolar configuration with particles aligned parallel to the droplet interface or a homogeneous configuration with particles aligned parallel to the long axis of the tactoid. Here, we report the first observation of the continuous transition in shape and director-field configuration of tactoids in true solutions of carbon nanotubes in chlorosulfonic acid. This observation is possible because the exceptional length of carbon nanotubes shifts the transition to a size range that can be visualized by optical microscopy. Polarization micrographs yield the interfacial and elastic properties of the system. Absorbance anisotropy measurements provide the highest nematic order parameter ($S = 0.79$) measured to date for a nematic phase of carbon nanotubes at coexistence with its isotropic phase.

DOI: 10.1103/PhysRevE.91.042507 PACS number(s): 64.70.M−, 61.30.Cz, 82.70.Dd

I. INTRODUCTION

The shape of the interfaces between simple fluids such as water and oil is solely governed by interfacial tension. In complex fluids such as liquid crystals, interfacial shape is controlled by the competition of interfacial tension and bulk elasticity, which in turn depend on the molecular orientation and alignment. A good example of this competition is the spindle shape of nematic droplets (tactoids) coexisting with the isotropic phase in liquid crystals [1,2] [Fig. 1(a)].

Tactoids have been observed for over a hundred years in fluids containing highly elongated colloids or macromolecules [2–9]. So far, the observed tactoids have displayed only a bipolar configuration, where the director field (representative of the local molecular orientation) is parallel to the interface and converges at two surface point defects called boojums [Fig. 1(b)] [2–6,10,11], with the exception of the recent report of homogeneous tactoids [uniform director field, Fig. 1(c)] in aqueous carbon nanotube (CNT) suspensions [9]. Yet, macroscopic theory predicts that tactoids should display a continuous range of configurations from homogeneous toward bipolar, including intermediate configurations, where the boojums are outside the droplet [virtual boojums, Fig. 1(d)]. The shape of the tactoids as described by the aspect ratio R/r varies from almost needle-like in the limit of small size to spheroidal in the limit of large size, where R and r are the length of the major and minor axes [Fig. 1(c)]. Large and small are relative to a length scale set by the elastic and surface properties of the nematic and hence on the dimensions of the molecules (see Sec. III A). The director-field configuration of the tactoid is described by the bipolarness ratio $R/\tilde{R}$, where $\tilde{R} \geq R$ is the distance between the boojums. Here, we present the first experimental evidence of the gradual transition from a homogeneous ($\tilde{R} \to \infty$) to a bipolar ($\tilde{R} = R$) configuration and from a very elongated toward a spheroidal shape in tactoids of CNTs in chlorosulfonic acid (CSA). By fitting macroscopic theory to our experimental data, we extract information on the elastic and surface properties of the nematic. We also determine the scalar order parameter of nematic phase of CNTs in CSA using absorption measurements.

II. MATERIALS AND TECHNIQUES

We used a solution of double and triple-walled CCNI CNTs (Continental Carbon Nanotechnologies, Inc.) (1000 ppm by weight) in CSA (99% purity, purchased from Sigma Aldrich). The prepared solutions were speed mixed (DAC 150.1 FV-K, Flack Tek Inc.) for 2.5 h, followed by stir bar mixing for 24 h and bath sonication (Bransonic M1800) for 25 h. The CNT length after sonication was $L \approx 1$ μm. The solution was loaded into rectangular glass capillaries (0.2 $\times$2 mm, used as received), which were flame sealed at the ends to

*These authors contributed equally to this work.
†Author to whom correspondence should be addressed: mp@rice.edu

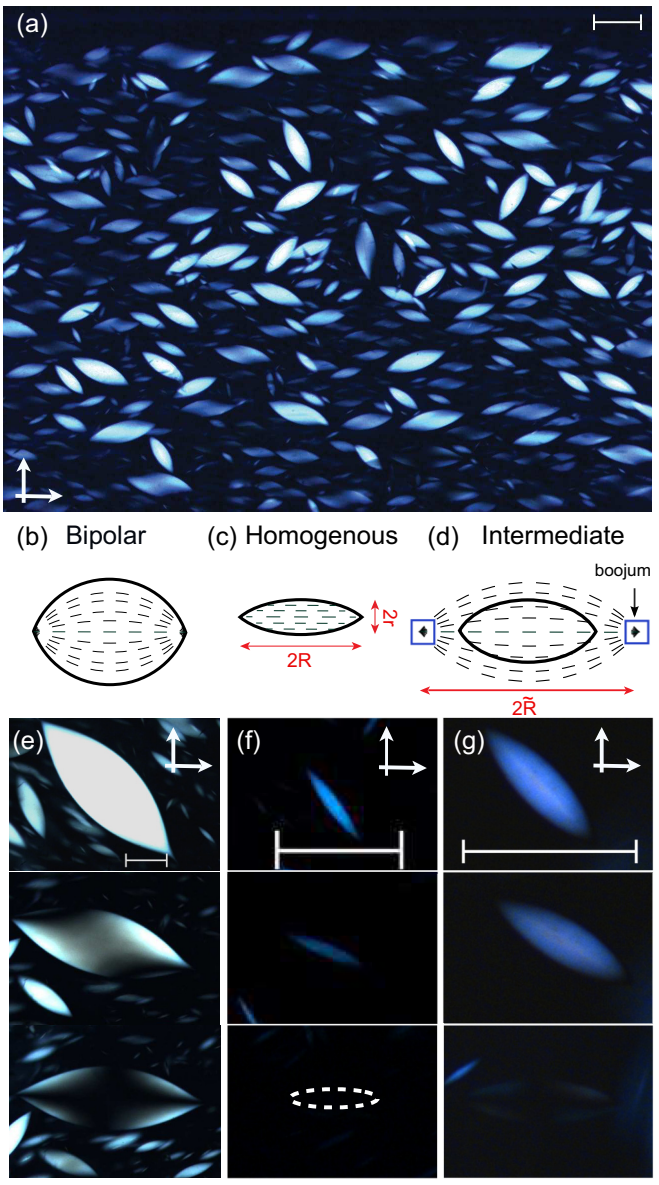

FIG. 1. (Color online) Nematic tactoids of different configurations formed in a solution of carbon nanotubes in chlorosulfonic acid at 1000 ppm. (a) Polarized optical micrograph showing a collection of tactoids of various size and extinction pattern related to the director-field configuration. Arrows show the orientation of crossed polarizers. Schematic representation of (b) bipolar, with boojum surface defects at the poles, (c) homogenous, and (d) intermediate tactoids characterized by virtual boojums outside of the droplet. R and r denote the major and minor axes of the tactoid, respectively. (e) Optical texture of a bipolar tactoid at the brightest transmission at 45° with respect to the polarizers (top), two dark brushes appearing toward the interface as tactoid is rotated (middle) and a dark cross at the center with bright lobes close to the droplet interface when parallel to either of the polarizers (bottom). (f) Optical texture of a homogeneous tactoid with a uniform change in brightness as it rotates away from 45° (top to bottom). (g) Optical texture of an intermediate tactoid with a nonuniform brightness change (top to bottom) and a low-contrast cross at the center (bottom). All the scale bars are 100 μm.

prevent exposure to humidity in air. In order to let our system reach equilibrium, the sealed capillaries were allowed to rest for 15 days. From the thermodynamic perspective, tactoids are structures in local equilibrium that form at the isotropic-nematic coexistence. Therefore, we can measure the shape, size, and director-field configuration of tactoids any time after they reach local equilibrium associated with the minimum free energy. Note that the system is kinetically evolving with tactoids coalescing to form two continuous phases at the global thermodynamic equilibrium. The two separated nematic and isotropic phases may only be achieved after years (two-year-old capillaries contain a few giant tactoids and few small tactoids). We measured the major and minor axes and the director field configuration of more than two hundred tactoids using polarizing optical microscopy (Fig. 1) [Zeiss AxioPlan 2 and a 10×(NA = 0.2) dry objective]. Images were recorded with a cooled charge-coupled device (CCD) camera (AxioCam Zeiss). All the size and shape determinations were performed using ImageJ software package (available from the National Institute of Health website) by fitting an ellipse that envelopes a tactoid. Optical absorption spectra of a CNT nematic were measured through a pinhole of 10 μm (Thorlabs, Inc.) using a spectrometer USB 2000 (OceanOptics) and a 100×(NA = 1.4) oil objective mounted on an Olympus inverted microscope X81. Birefringence at $\lambda = 546$ nm was determined using a Berek compensator (Olympus).

III. RESULTS AND DISCUSSIONS

A. Shape and Director field of tactoids

The director-field ($\mathbf{n}(\mathbf{r})$) configurations were determined by imaging tactoids at different orientations between crossed polarizers and classifying the optical textures based on literature on bipolar [2,10] and homogenous [9] tactoids, as well as Jones matrix calculations [12] of tactoids with representative configurations. Optical textures were simulated using size (R) and shape (R/r) measurements of the tactoids at 1000 ppm in Figs. 1(e)–1(g) and 2, and birefringence Δn estimated approximately for this concentration using the Michel-Levy interference color chart. Figure 2 shows experimental and simulated optical textures of tactoids with $R/\tilde{R}$ of 1 (bipolar), 0 (homogenous), and 0.75 (intermediate), and their major axis rotated clockwise with respect to a polarizer by 0°, 15°, 30°, and 45°. Bipolar tactoids show four dark brushes crossing at the center when either of the crossed polarizers is aligned with the major axis of the tactoid. By rotating the tactoid, the dark cross splits into two dark curved brushes that move away from each other [Fig. 1(e)]. Homogenous tactoids show a uniform change in brightness when the tactoid is rotated from 0° to 45° relative to either of the polarizers, and are uniformly dark at 0° [Fig. 1(f)]. Intermediate tactoids show a nonuniform optical texture upon rotation, and low-contrast crossed brushes spread over most of the tactoid area when either of the polarizers is aligned along the tactoid axis [Fig. 1(g)]. Textures of homogeneous tactoids have a mirror symmetry with respect to planes perpendicular to the field of view and going along a major or minor axis at any rotation angle with respect to crossed polarizers [Fig. 2(b)]. Textures of bipolar and intermediate tactoids have the same mirror

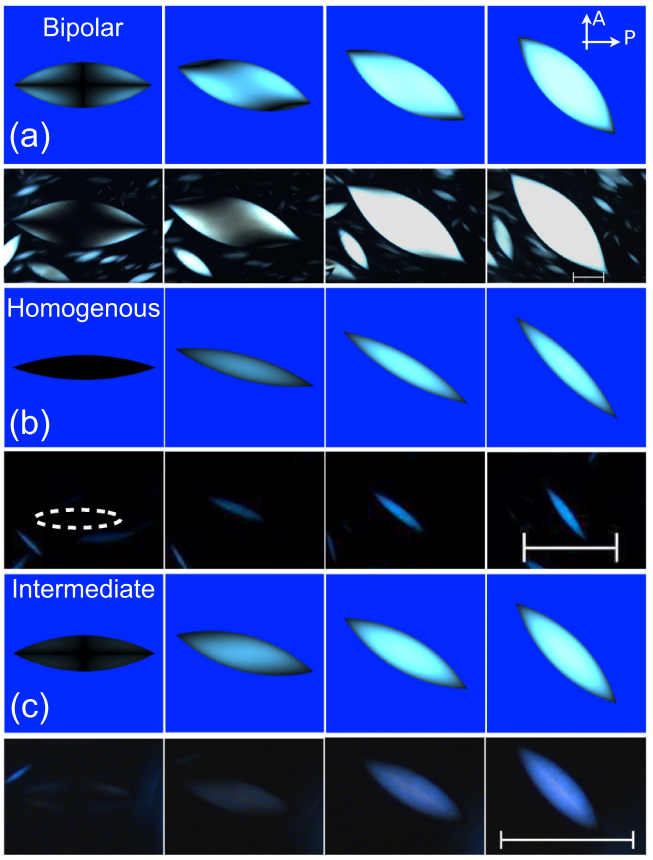

FIG. 2. (Color online) Experimental (at 1000 ppm) and simulated (at $\Delta n = 0.0019$) polarized micrographs of bipolar, homogenous, and intermediate tactoids as rotated between crossed polarizers. (a) In a bipolar tactoid ($R/r = 3.0$) the director lines converge on the droplet cusps ($\tilde{R} = R$), (b) in a homogenous tactoid ($R/r = 5.7$) director field lines converge at infinity ($\tilde{R} \to \infty$). (c) The intermediate configuration ($R/r = 3.9$) is a results of a gradual movement of boojums toward the droplet cusps. All the scale bars are 100 μm.

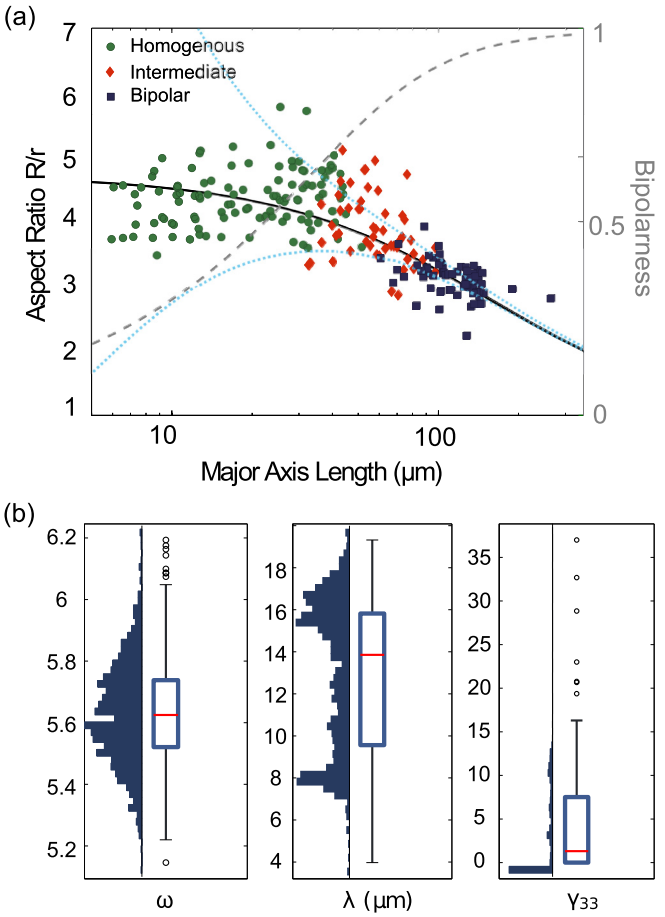

FIG. 3. (Color online) Tactoid size and shape measurements and statistical analysis. (a) Aspect ratio and director field as a function of major axis length of 229 tactoids. The solid black line shows the theoretical prediction with the median bootstrap parameters $\omega = 5.6$, $\lambda = 13.9$ μm, and $\gamma_{33} = 1.3$. The dashed line shows the predicted level of bipolarness of the director field described by the relative length of the tactoids and the distance between the virtual boojums. The dotted blue lines show the upper and lower 95% confidence interval on the aspect ratio; see Appendix A. (b) Box plots show distribution of the bootstrapped parameters ω, λ, and γ_{33} with marginal histogram of each parameter. Each box plot is based on fitting the theory to 1000 random resampling of the original data set shown in panel (a). The top and bottom edges of the boxes denote the upper and lower quartiles, solid red lines show the medians, open circles show the outliers, and whiskers show the most extreme points within 1.5 times of the interquartile range.

symmetry only when at an angle of 0°, ±45°, and ±90° to the polarizer; at other orientations they both have inversion symmetry with respect to the center of the tactoid [Figs. 2(a) and 2(c)]. The difference between the optical texture of a bipolar and intermediate tactoid is that the ends of the dark brushes along the major axis appear much sharper in the cusps of bipolar tactoids because the director field lines converge on the droplet poles [Fig. 1(b)]; ends of a brush along the major axis of the intermediate tactoid do not converge on the poles but spread across cusps.

Figure 3(a) summarizes measurements on size, shape, and configuration of a set of tactoids. Small tactoids ($R < 35$ μm, green circles) display a homogeneous director field, intermediate-size tactoids ($35 < R < 90$ μm, red diamonds) display an intermediate director field, and large tactoids ($R > 90$ μm, purple squares) are bipolar. These observations demonstrate that the whole range of tactoid morphologies can be observed in a single sample. As tactoids grow larger, their shape crosses over from highly elongated with an average aspect ratio of ≈5 to spheroidal with smallest observed aspect ratio of ≈2. Our largest tactoids are comparable in size to the thickness of the capillary (200 μm) and hence we do not expect to see spherical tactoids in our system.

The equilibrium shape (described by the unit surface normal $\mathbf{q}$) and director-field configuration (described by the unit vector $\mathbf{n}$) minimize the sum of elastic and surface free energies [1]:

$$F = \int_V dV \left[\frac{1}{2}k_{11}(\nabla\cdot\mathbf{n})^2 + \frac{1}{2}k_{33}[\mathbf{n}\times(\nabla\times\mathbf{n})]^2\right] - \int_V dV k_{24}\nabla\cdot[\mathbf{n}\nabla\cdot\mathbf{n} + \mathbf{n}\times(\nabla\times\mathbf{n})] + \int_A dA[\tau + W(\mathbf{q}\cdot\mathbf{n})^2], \quad (1)$$

where V and A are, respectively, the volume and area of the tactoid; k_{11}, k_{33}, and k_{24} are, respectively, the splay, bend, and saddle-splay Frank elastic constants; τ is the interfacial tension between the isotropic phase and the nematic phase when the molecules are aligned parallel to the interface; and W is the surface anchoring strength and accounts for the effect of nonplanar molecular orientation on interfacial tension. Polarizing microscopy textures (Fig. 1) indicate that CNTs prefer planar anchoring ($W > 0$) at the interface as expected from theory and simulations [13–16]. The equilibrium shape of a tactoid can be computed by minimizing the free energy F at a fixed value of the volume V. Rather than doing an unconstrained minimization, we follow Prinsen and van der Schoot [1] and assume a bispherical director field and axial symmetry that capture the shape of our tactoids. The optimization is then with respect to the aspect ratio and bipolarness of the director field.

It is convenient to group free-energy parameters into $\lambda \equiv (k_{11} - k_{24})/\tau\omega$, $\omega \equiv W/\tau$, and $\gamma_{33} \equiv k_{33}/(k_{11} - k_{24})$—for a symmetric tactoid k_{24} merely rescales k_{11} [1]. A scaling analysis of Eq. (1) shows that λ is the extrapolation length that controls the crossover from elasticity-dominated alignment (homogeneous) to anchoring-dominated alignment (bipolar) [1]. The magnitude of ω determines the aspect ratio of the tactoids in the limit of small size corresponding to a homogenous director field configuration [17]. The influence of γ_{33}, which measures the relative strength of the bend and splay elasticity, is expected to be the greatest for bipolar tactoids, where the competition between splay and bend deformation energies versus surface energy determines the shape [1].

We obtained λ, ω, and γ_{33} by a global least-squares fit to the measured aspect ratio versus size (see Ref. [1] for details of the theory) and compared our experimental results to theoretical predictions for the director-field configurations. Note that there is scatter in the data related to experimental accuracy and the slow time evolution of the tactoids; see Appendix A. We performed a "bootstrap" statistical analysis to compute confidence intervals on the parameters [18]. The original data set shown in Fig. 3(a) was resampled 1000 times by drawing data points randomly from the set with replacement. Fitting the theory to the resampled data sets generates a probability distribution for the parameters along with the marginal histograms [Fig. 3(b)].

Box plots in Fig. 3(b) show the median (red line), the median of the lower and the upper half of the data set (the lower and the upper quartiles, the blue edges of the box), and 1.5 times of the distance between the lower and the upper quartiles (black whiskers). The open circles in the graphs indicate outliers that are not within the indicated ranges. For example, the distribution of dimensionless anchoring strength ω shows that within a 50% confidence interval (CI), the value must be between 5.5 and 5.7 with the median of 5.6. Within a 99% CI (presuming a normal distribution), the value ranges between 5.2 and 6. The theoretical prediction for the aspect ratio and the director-field configuration are plotted in Fig. 3(a) (solid and dashed lines, respectively) with the median bootstrap values of the parameters ($\lambda \approx 13.9$ μm, $\omega \approx 5.6$, and $\gamma_{33} \approx 1.3$). The theoretical predictions are consistent with the trend of the data, including the onset of the crossover from homogenous toward bipolar ($R/\tilde{R} = 0.5$) at a major axis size of 35 μm.

We are able to observe this crossover because of the very large extrapolation length associated with our specific system (λ bootstrap median ≈ 13.9 μm, $2R_{\text{crossover}} \propto \lambda$). Theoretically, we can show that for monodisperse hard rods, we expect $\lambda \approx 13L$; see Appendix B. The CNTs used in this study have $L \approx 1$ μm, longer than particles used elsewhere. This explains why in the literature almost only bipolar tactoids have been observed [1,2,6,10]. However, we note that the elastic and surface properties of the coexisting phases are sensitive to the type of molecular interactions, flexibility, and polydispersity; hence, this prefactor may change for a polydisperse system where the nematic phase is enriched with longer rods.

The only study that showed homogenous tactoids is that of bile salt-stabilized CNTs in water by Puech *et al.* [9]. However, their experimental system was 10–20 μm wide and only yielded small tactoids below the crossover size with homogenous director fields [19]. Their reported value ($\omega = 4$) is comparable to our estimate of $\omega \approx 5.6$ [bootstrap median, 99% CI = 5.2 to 6; see Fig. 3(b)]. Both of these values are larger than the theoretical predictions for the dimensionless anchoring strength $0.5 \lesssim \omega \lesssim 1.5$ of rod-like particles, allowing for varying bending flexibility [13–15,20,21]. A plausible candidate for this discrepancy is length polydispersity. In length polydisperse systems the longer rods accumulate in the nematic phase and preferentially lie along the interface [15].

Bipolar tactoids have been observed in a variety of systems [2–6,8]. In a few cases, the theory is fitted to the size measurements [1,2,6,10]. However, because of the limited number of data points, the absence of a proper statistical analysis, and a data set that does not cover all of the director-field configurations, only lower estimates for ω could be obtained ranging from about 10 to infinity [1,2,6,10]. For these systems, values of $\omega\lambda$ range from 1 to 8 μm, which is well below our measured value of $\lambda\omega \approx 78$ μm, explaining once again why the crossover toward homogenous regime has not been observed so far. Furthermore, using data sets that fail to cover spherical shape limit can result in uncertain values of γ_{33} [1], implying that the uncertainty in our value [bootstrap γ_{33} median ≈ 1.3, 99% CI = 0 to 16.3, see Fig. 3(b)] and the values obtained in these studies are large. Values of γ_{33} reported in the literature range from 20 to 60 [1,2,6,10], which fall in the outlier region for our measurements [see Fig. 3(b)].

B. Order parameter and optical properties of nematic phase in tactoids

In our system, tactoids are large enough to investigate the average alignment of CNTs in a nematic phase (described by the scalar order parameter S). CNTs are optically uniaxial [22] and so is the nematic phase; therefore, the level of alignment can be determined by measuring the absorption anisotropy [22–24] of the CNT nematic. We measure absorption spectra for light polarized parallel $A_{||}$ and perpendicular $A_{\perp}$ to the major axis (Fig. 4) and determine the scalar order parameter via $S = (A_{||} - A_{\perp})/(A_{||} + 2A_{\perp})$ [23,24]. The absorption spectra are measured in the uniformly aligned central part [see schematics of $\mathbf{n}(\mathbf{r})$ in Figs. 1(b)–1(d)] of tactoids formed in 3000 ppm by weight solution of CNTs in CSA in a 200 μm capillary [Fig. 4(a)]. Results for the parallel and the perpendicular orientations are shown in Fig. 4(b). The scalar

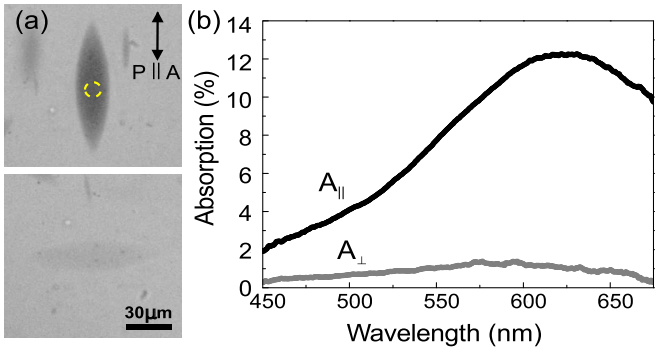

FIG. 4. (Color online) Order parameter measurement in tactoids using absorption anisotropy. (a) Optical textures of a CNT tactoid at 3000 ppm obtained between parallel polarizers "P" and "A" with its major axis oriented parallel (top) and perpendicular (bottom) to the polarizers. (b) Optical absorption spectra for nematic phase in solution of CNT in CSA measured at the center of the tactoid [yellow circle in panel (a)].

order parameter evaluated at the maximum parallel absorption $A_{||}$ at the wavelength of $\lambda = 622$ nm gives a value of $S = 0.79$. Using the integrated absorptions over the measured absorption band from 450 to 700 nm results in a similar value of $S = 0.74$. The scalar order parameter measured here is slightly larger than the values measured for other systems of rod-like particles at coexistence [25–28].

The measured value is consistent with predictions of the Onsager model that yields an order parameter of about 0.79 for monodisperse hard rods at coexistence [29–31]. However, our system deviates from the classical Onsager-like hard-rod model in two ways. First, our CNTs do not interact via a hard-core potential; the CSA solvent charges the CNTs and stabilizes them against the van der Waals attractions [32]. Second, our system is polydisperse, in particular in length; no reliable estimate is available for the nematic order parameter in polydisperse rod-like systems at coexistence. The theoretical predictions give values very close to unity [33,34]; however, these estimates are based on approximate orientational distribution functions known to vastly overestimate the order parameter at coexistence.

We also probe an optical birefringence of a CNT nematic in tactoids, which is a macroscopic property closely related to the order parameter of the tubes. The optical birefringence of a well-aligned nematic is defined as $\Delta n = n_{||} - n_{\perp}$, where $n_{||}$ and $n_{\perp}$ are refractive indices measured for light polarized, respectively, parallel and perpendicular to the main optical axis of the nematic. The optical birefringence in the first approximation is proportional to the microscopic order parameter of the nematic phase as $|\Delta n| \propto S$ [35] and depends on concentration of nanotubes [22]. We measured $\Delta n \approx 0.0044$–0.0062 for the nematic phase in tactoids formed in CNTs-CSA solution at slightly higher concentration of 3000 ppm by weight using a Berek compensator (Olympus) at $\lambda = 546$ nm. The obtained values are within the range of birefringence measured previously in water-based suspensions of CNTs at different concentrations and aligned by a shear flow [22]. The difference of optical birefringence measured for tactoids of different size was within an error of measurements by the Berek compensator we used, which allows us to conclude that it is independent of the size of tactoids in the measured range of sizes (tens of microns) and is determined by the CNT concentration and the order parameter.

IV. CONCLUSION

We have shown that nematic tactoids with a high degree of orientational order emerge in solutions of very long CNTs in CSA. We have, to our knowledge, revealed for the first time the crossover in the director field from homogenous toward bipolar corresponding to shape transition from highly elongated toward spheroidal. Direct comparison of our observations with macroscopic theory enabled us to estimate the anchoring strength of the director field to the isotropic-nematic interface, the ratio of the bend and splay elastic constants, as well as the so-called extrapolation length that measures the relative strength of the elastic and surface forces. Optical probing of the crossover is only possible if the extrapolation length is large, which requires the rod-like particles to be sufficiently long, as is the case for our CNTs.

In addition to an intrinsic fundamental interest, CNT tactoids hold great potential technological relevance. A high degree of CNT alignment, in conjunction with the spatial uniformity of such alignment, are crucial for realizing the exceptional properties of CNT in macroscopic materials. For example, wet spinning of CNT liquid crystalline has proved to be effective in forming highly aligned, continuous CNT fibers with high strength and conductivity [36], while biphasic solutions of CNTs in acids have been shown to yield highly conductive, transparent films [37]. Nematic CNT tactoids offer an easily accessible liquid crystal monodomain for studying and understanding the morphology of the CNT solutions, which is key to future improvements of processing and properties of macroscopic CNT materials.

ACKNOWLEDGMENTS

This work was financially supported by Teijin Aramid, Air Force Office of Scientific Research (Grant No. FA9550-09-1-0590), the Welch Foundation (Grant No. C-1668), and US Department of Energy, Office of Basic Energy Sciences, Division of Materials Sciences and Engineering grants. B.S. acknowledges the support of ICAM Branch Contributions. J.A.L. was supported by the National Science Foundation Nanoscale Science and Engineering Center under Grants No. CMMI-0531171 and No. CMMI-1031171. We thank Dr. Philippe Poulin, Peter Prinsen, and Robert Pinnick for helpful comments.

APPENDIX A: SOURCES OF INACCURACY IN TACTOID SIZE MEASUREMENTS

There are some sources of uncertainty in our measurements that can be attributed to the following reasons. Deviation from the local equilibrium condition is observed during the relaxation of a shape of a tactoid after coalescence. This inaccuracy predominantly contributes to the large size limit due to the slower relaxation of large tactoids. The inaccuracy can also be the result of the susceptibility of the aspect ratio to thermal fluctuations, because of the low interfacial tension

between the coexisting isotropic and nematic phases, of the order nN/m [38]. Using Boltzmann probability distribution for the free energy of the tactoids, the 95% confidence interval on the aspect ratio is plotted in Fig. 3(a) using an estimated value of surface tension 0.5 nN/m. Theoretically, we expect the smaller tactoids to exhibit a larger spread due to the smaller interfacial areas and hence lower surface free energies. Even though the estimated value of surface tension might not be exact and further experiments are required to measure surface tension, decreasing the surface tension would only widen the envelope without any change in the trend. There is a measurement inaccuracy that contributes mostly to small tactoids (few microns long), where it becomes difficult to find the exact location of the tips and fit an ellipse that passes through them. Additionally, if tactoids are tilted within the capillary (along their minor axis), they appear symmetric from the top. Here, we tried to avoid this source of inaccuracy by only measuring tactoids with both tips in focus. The last source of inaccuracy is due to small retardation near the edges of the tactoid. When the tactoids are imaged in their brightest transmission (tactoid axis at 45° inclined with respect to the polarizers), their cusps are darkened resulting in up to 10% underestimation in major axis length and hence the aspect ratio. Note that this underestimation might not be the same for all the tactoids because of the possible difference in the level of exposure among the images.

APPENDIX B: SCALING ANALYSIS ON EXTRAPOLATION LENGTH

Using the theoretical expressions for splay elastic constant k_{11} [39], surface tension τ [40], and dimensionless surface anchoring ω [21], we estimate the dependency of λ on the dimensions of the constitutive molecules of a monodisperse system. The molecules are assumed to be cylinders of diameter D and length L. The dimensionless splay elastic constant $k_{11}D/k_BT$ is estimated to be $7/(8\pi)c_a$, where c_a is the number density of the nematic phase scaled with respect to the isotropic excluded volume, and k_B is a Boltzmann constant [39]. The nematic phase density c_a at the coexistence is calculated numerically by Lekkerkerker *et al.* [41] and gives $c_a = 4.191$. The dimensionless surface tension of the isotropic-nematic interface for a monodisperse hard-rod system is $\tau DL/k_BT = 0.156$ [40]. The dimensionless anchoring for rigid rods are expected to be 0.58 [21]. Hence, the ratio $k_{11}/\tau\omega$ is equal to $\approx 13L$. Therefore, for the crossover to be observable in an optical microscope (micron scale resolution) the constitutive molecules should be few microns long. Note that this prefactor is highly sensitive to the properties of the coexisting phases including flexibility of the molecules, types of interactions, and polydispersity. For example, in a length polydisperse system, the longer rods accumulate in the nematic phase and contribute to the larger anisotropy of the surface tension.

[1] P. Prinsen and P. van der Schoot, Continuous director-field transformation of nematic tactoids, Eur. Phys. J. E **13**, 35 (2004).

[2] A. V. Kaznacheev, M. M. Bogdanov, and A. S. Sonin, The influence of anchoring energy on the prolate shape of tactoids in lyotropic inorganic liquid crystals, J. Exp. Theoret. Phys. **97**, 1159 (2003).

[3] H. Zocher, Über freiwillige Strukturbildung in Solen, Z. Anorg. Allg. Chem. **147**, 91 (1925).

[4] F. C. Bawden, N. W. Pirie, J. D. Bernal, and I. Fankuchen, Liquid crystalline substances from virus-infected plants, Nature **138**, 1051 (1936).

[5] J. D. Bernal and I. Fankuchen, X-ray and crystallographic studies of plant virus preparations I. Introduction and preparation of specimens II. Modes of aggregation of the virus particles, J. Gen. Physiol. **25**, 111 (1941).

[6] A. V. Kaznacheev, M. M. Bogdanov, and S. A. Taraskin, The nature of prolate shape of tactoids in lyotropic inorganic liquid crystals, J. Exp. Theoret. Phys. **95**, 57 (2002).

[7] Z. Dogic, Surface freezing and a two-step pathway of the isotropic-smectic phase transition in colloidal rods, Phys. Rev. Lett. **91**, 165701 (2003).

[8] J. Viamontes, P. W. Oakes, and J. X. Tang, Isotropic to nematic liquid crystalline phase transition of *F*-actin varies from continuous to first order, Phys. Rev. Lett. **97**, 118103 (2006).

[9] N. Puech, E. Grelet, P. Poulin, C. Blanc, and P. van der Schoot, Nematic droplets in aqueous dispersions of carbon nanotubes, Phys. Rev. E **82**, 020702 (2010).

[10] P. W. Oakes, J. Viamontes, and J. X. Tang, Growth of tactoidal droplets during the first-order isotropic to nematic phase transition of F-actin, Phys. Rev. E **75**, 061902 (2007).

[11] M. Kleman and O. D. Lavrentovich, Topological point defects in nematic liquid crystals, Philos. Mag. **86**, 4117 (2006).

[12] P. Yeh and C. Gu, *Optics of Liquid Crystal Displays*, Vol. 67 (John Wiley & Sons, New York, 2010).

[13] Z. Y. Chen and J. Noolandi, Numerical solution of the Onsager problem for an isotropic-nematic interface, Phys. Rev. A **45**, 2389 (1992).

[14] D. L. Koch and O. G. Harlen, Interfacial tension at the boundary between nematic and isotropic phases of a hard rod solution, Macromolecules **32**, 219 (1999).

[15] P. van der Schoot, Remarks on the interfacial tension in colloidal systems, J. Phys. Chem. B **103**, 8804 (1999).

[16] A. J. McDonald, M. P. Allen, and F. Schmid, Surface tension of the isotropic-nematic interface, Phys. Rev. E **63**, 010701 (2000).

[17] A. Rapini and M. Papoular, Distorsion d'une lamelle nématique sous champ magnétique conditions d'ancrage aux parois, J. Phys. (Paris) Colloques **30**, C4-54 (1969).

[18] B. Efron, Bootstrap methods: another look at the jackknife, Ann. Stat. **7**, 1 (1979).

[19] P. Poulin (private communication).

[20] S.-M. Cui, O. Akcakir, and Z. Y. Chen, Isotropic-nematic interface of liquid-crystalline polymers, Phys. Rev. E **51**, 4548 (1995).

[21] Y. Jiang and J. Z. Y. Chen, Isotropic-nematic interface in a lyotropic system of wormlike chains with the Onsager interaction, Macromolecules **43**, 10668 (2010).

[22] D. Fry, B. Langhorst, H. Wang, M. L. Becker, B. J. Bauer, E. A. Grulke, and E. K. Hobbie, Rheo-optical studies of carbon nanotube suspensions, J. Chem. Phys. **124**, 054703 (2006).

[23] Y. A. Nastishin, H. Liu, T. Schneider, V. Nazarenko, R. Vasyuta, S. V. Shiyanovskii, and O. D. Lavrentovich, Optical characterization of the nematic lyotropic chromonic liquid crystals: Light absorption, birefringence, and scalar order parameter, Phys. Rev. E **72**, 041711 (2005).

[24] B. Dan, N. Behabtu, A. Martinez, J. S. Evans, D. V. Kosynkin, J. M. Tour, M. Pasquali, and I. I. Smalyukh, Liquid crystals of aqueous, giant graphene oxide flakes, Soft Matter **7**, 11154 (2011).

[25] N. Puech, C. Blanc, E. Grelet, C. Zamora-Ledezma, M. Maugey, C. Zakri, E. Anglaret, and P. Poulin, Highly ordered carbon nanotube nematic liquid crystals, J. Phys. Chem. C **115**, 3272 (2011).

[26] R. Oldenbourg, X. Wen, R. B. Meyer, and D. L. D. Caspar, Orientational distribution function in nematic tobacco-mosaic-virus liquid crystals measured by X-Ray diffraction, Phys. Rev. Lett. **61**, 1851 (1988).

[27] E. Grelet and S. Fraden, What is the origin of chirality in the cholesteric phase of virus suspensions?, Phys. Rev. Lett. **90**, 198302 (2003).

[28] N. Puech, M. Dennison, C. Blanc, P. van der Schoot, M. Dijkstra, R. van Roij, P. Poulin, and E. Grelet, Orientational order of carbon nanotube guests in a nematic host suspension of colloidal viral rods, Phys. Rev. Lett. **108**, 247801 (2012).

[29] L. Onsager, The effects of shape on the interaction of colloidal particles, Ann. NY Acad. Sci. **51**, 627 (1949).

[30] G. Lasher, Nematic ordering of hard rods derived from a scaled particle treatment, J. Chem. Phys. **53**, 4141 (1970).

[31] S.-D. Lee and R. B. Meyer, Computations of the phase equilibrium, elastic constants, and viscosities of a hard-rod nematic liquid crystal, J. Chem. Phys. **84**, 3443 (1986).

[32] M. J. Green, A. N. G. Parra-Vasquez, N. Behabtu, and M. Pasquali, Modeling the phase behavior of polydisperse rigid rods with attractive interactions with applications to single-walled carbon nanotubes in superacids, J. Chem. Phys. **131**, 084901 (2009).

[33] H. H. Wensink and G. J. Vroege, Isotropic-nematic phase behavior of length-polydisperse hard rods, J. Chem. Phys. **119**, 6868 (2003).

[34] A. Speranza and P. Sollich, Isotropic-nematic phase equilibria of polydisperse hard rods: the effect of fat tails in the length distribution, J. Chem. Phys. **118**, 5213 (2003).

[35] P.-G. De Gennes and J. Prost, *The Physics of Liquid Crystals*, Vol. 23 (Clarendon Press, Oxford, 1993).

[36] N. Behabtu, C. C. Young, D. E. Tsentalovich, O. Kleinerman, X. Wang, A. W. K. Ma, E. A. Bengio, R. F. ter Waarbeek, J. J. de Jong, R. E. Hoogerwerf, S. B. Fairchild, J. B. Ferguson, B. Maruyama, J. Kono, Y. Talmon, Y. Cohen, M. J. Otto, and M. Pasquali, Strong, light, multifunctional fibers of carbon nanotubes with ultrahigh conductivity, Science **339**, 182 (2013).

[37] F. Mirri, A. W. K. Ma, T. T. Hsu, N. Behabtu, S. L. Eichmann, C. C. Young, D. E. Tsentalovich, and M. Pasquali, High-performance carbon nanotube transparent conductive films by scalable dip coating, ACS Nano **6**, 9737 (2012).

[38] R. van Roij, The isotropic and nematic liquid crystal phase of colloidal rods, Eur. J. Phys. **26**, S57 (2005).

[39] T. Odijk, Elastic constants of nematic solutions of rod-like and semi-flexible polymers, Liquid Crystals **1**, 553 (1986).

[40] K. Shundyak and R. van Roij, Isotropic-nematic interfaces of hard-rod fluids, J. Phys. Cond. Matt. **13**, 4789 (2001).

[41] H. N. W. Lekkerkerker, P. Coulon, R. Van der Haegen, and R. Deblieck, On the isotropic-liquid crystal phase separation in a solution of rodlike particles of different lengths, J. Chem. Phys. **80**, 3427 (1984).